

January 01, 1998

Compton study of Ni₇₅Cu₂₅ and Ni₇₅Co₂₅ disordered alloys: Theory and experiment

A. Bansil

Northeastern University

S. Kaprzyk

Academy of Mining and Metallurgy

A. Andrejczuk

Warsaw University Branch in Bialystok

L. Dobrzynski

Warsaw University Branch in Bialystok

J. Kwiatkowska

Institute of Nuclear Physics

See next page for additional authors

Recommended Citation

Bansil, A.; Kaprzyk, S.; Andrejczuk, A.; Dobrzynski, L.; Kwiatkowska, J.; Maniawski, F.; and Zukowski, E., "Compton study of Ni₇₅Cu₂₅ and Ni₇₅Co₂₅ disordered alloys: Theory and experiment" (1998). *Physics Faculty Publications*. Paper 365.

Author(s)

A. Bansil, S. Kaprzyk, A. Andrejczuk, L. Dobrzynski, J. Kwiatkowska, F. Maniawski, and E. Zukowski

Compton study of $\text{Ni}_{75}\text{Cu}_{25}$ and $\text{Ni}_{75}\text{Co}_{25}$ disordered alloys: Theory and experiment

A. Bansil

Department of Physics, Northeastern University, Boston, Massachusetts 02115

S. Kaprzyk

*Faculty of Physics and Nuclear Techniques, Academy of Mining and Metallurgy, al.Mickiewicza 30, 30059 Kraków, Poland
and Department of Physics, Northeastern University, Boston, Massachusetts 02115*

A. Andrejczuk and L. Dobrzyński

Institute of Physics, Warsaw University Branch in Białystok, Lipowa 41, Poland

J. Kwiatkowska and F. Maniowski

Institute of Nuclear Physics, Cracow, Radzikowskiego 152, Poland

E. Żukowski

Institute of Physics, Warsaw University Branch in Białystok, Lipowa 41, Poland

(Received 23 July 1997)

We present first-principles computations of ferromagnetic electronic structures and spin-resolved Compton profiles along the three high-symmetry directions in $\text{Ni}_{75}\text{Cu}_{25}$ and $\text{Ni}_{75}\text{Co}_{25}$ disordered alloys, together with the corresponding Compton measurements from single-crystal specimens with a ^{137}Cs source. The theoretical results are based on the use of the charge- and spin-self-consistent Korringa-Kohn-Rostoker coherent-potential-approximation framework to treat disorder, and the local spin-density scheme for incorporating exchange-correlation effects; the lattice constants in all cases are obtained by minimizing the total energy. The majority-spin spectrum of Ni undergoes relatively small changes upon alloying with Cu or Co, and the associated majority-spin contribution to the Compton profiles of Ni, $\text{Ni}_{75}\text{Cu}_{25}$ and $\text{Ni}_{75}\text{Co}_{25}$ is nearly the same. In comparing theory and experiment, we focus on anisotropies in Compton profiles, and find the overall agreement with respect to the $J_{111}-J_{100}$, $J_{111}-J_{110}$, and $J_{110}-J_{100}$ anisotropies in $\text{Ni}_{75}\text{Cu}_{25}$ as well as $\text{Ni}_{75}\text{Co}_{25}$ to be reasonable, although some significant discrepancies around $p_z=0$ are notable. We show clearly that the momentum resolution of 0.4 a.u. (full width at half maximum) of the present experiment washes out some of the fine structure in the Compton spectra, and that these spectral features should be accessible via higher resolution measurements with a synchrotron light source. [S0163-1829(98)03401-8]

I. INTRODUCTION

The advent of third-generation light sources has brought a renewed interest in Compton scattering as a tool for investigating electronic structure and fermiology related questions in materials.¹⁻⁹ The Compton technique offers a number of intrinsic advantages over other spectroscopies in this regard. Being essentially a ground-state measurement, the Compton experiment does not require long electron mean free paths as is the case for transport-type experiments such as the $dHvA$, the latter being limited for this reason to systems with low defect and impurity concentrations. Since no charged particles go in or out of the sample, Compton is not complicated by surface effects present in photoemission or electron-scattering experiments, and is thus genuinely a bulk probe. Moreover, because light couples weakly to the electronic system, the disturbance of the electronic states one is trying to measure is relatively smaller in Compton compared to positron annihilation or photoemission-type spectroscopies that involve charged particles. Despite these advantages, the usefulness of Compton has been limited in actual applications based on the traditional γ -ray sources due to lack of adequate momentum resolution. Additionally, since all elec-

trons contribute to the Compton spectrum, the part associated with valence electrons, often of primary interest, sits atop the core contribution, and one thus faces a low signal-to-background problem, especially in high-Z materials. The availability of high energy, high intensity synchrotron sources should ameliorate these difficulties endemic to the Compton method, and make it possible to apply the technique more widely.

This article discusses Compton profiles of $\text{Ni}_{75}\text{Cu}_{25}$ and $\text{Ni}_{75}\text{Co}_{25}$ disordered alloys. New results are presented on the theoretical as well as the experimental side. Theoretical profiles are reported in $\text{Ni}_{75}\text{Cu}_{25}$, $\text{Ni}_{75}\text{Co}_{25}$, and the limiting case of Ni, within the Korringa-Kohn-Rostoker coherent-potential-approximation (KKR-CPA) framework.^{1,10-13} All computations include effects of magnetic ordering, and are parameter-free as these are based on lattice constants obtained by minimizing the total energy. A high level of charge- and spin-self-consistency is achieved in all cases. The existing theoretical Compton work on disordered alloys has been limited to a few nonself-consistent, nonmagnetic computations,¹⁴⁻¹⁶ although we have recently carried out an extensive self-consistent study of LiMg alloys.^{17,18} This work provides to our knowledge the first theoretical Comp-

ton profiles of a disordered magnetic alloy; these results constitute a reliable basis for testing the KKR-CPA and local spin-density (LSD) approximations that are the only significant assumptions underlying the present computations.

On the experimental side, we have carried out Compton measurements from single-crystal specimens of $\text{Ni}_{75}\text{Cu}_{25}$ and $\text{Ni}_{75}\text{Co}_{25}$ using the ^{137}Cs source. The motivation for considering these specific alloys was the thought that the Compton spectra of $\text{Ni}_{75}\text{Cu}_{25}$ and $\text{Ni}_{75}\text{Co}_{25}$ may differ rather substantially because Cu with full d bands is nonmagnetic and reduces the moment of Ni, while Co with open d shells increases the average moment in the alloy. Further, the number of electrons per unit cell in Ni increases on adding Cu, but decreases on adding Co. Despite these differences, we will see below that the Compton spectra of $\text{Ni}_{75}\text{Cu}_{25}$ and $\text{Ni}_{75}\text{Co}_{25}$ turn out not to differ as much as one might have guessed; higher resolution synchrotron-based Compton studies of these alloys would be interesting.

Concerning relevant literature beyond what has already been cited, we note that the CP's of Ni and Cu have been the subject of extensive theoretical computations as well as experimental studies using various γ -ray sources.^{19–29} CP's of $\text{Cu}_x\text{Ni}_{1-x}$ disordered alloys for mainly Cu-rich polycrystalline samples are reported in Ref. 15. The electronic structure of disordered $\text{Cu}_x\text{Ni}_{1-x}$ alloys has been the subject of numerous studies,^{30,31} but we are not aware of a previous charge- and spin-self-consistent *ab initio* study of the $\text{Ni}_{1-x}\text{Co}_x$ disordered alloys.

An outline of this article is as follows. The introductory remarks are followed by a brief discussion of computational details in Sec. II, and of the experimental aspects in Sec. III. The results for Compton spectra of Ni, $\text{Ni}_{75}\text{Cu}_{25}$, and $\text{Ni}_{75}\text{Co}_{25}$, and the relevant comparisons between theory and experiment are taken up in Sec. IV. Some concluding remarks are made in Sec. V.

II. COMPUTATIONAL DETAILS

The spin-dependent Compton profiles for $\text{Ni}_{75}\text{Cu}_{25}$ and $\text{Ni}_{75}\text{Co}_{25}$ disordered alloys are computed using the charge- and spin-self-consistent KKR-CPA methodology. The results for ferromagnetic Ni are based on KKR-CPA calculations in the single impurity limit, and were checked via completely independent KKR computations on ordered Ni. We refer to Refs. 13, 32, and 9 for a discussion of the underlying KKR-CPA formalism; the relevant Green function formulation for treating the momentum density and Compton profiles in disordered alloys is given in Refs. 33 and 34 and need not be repeated here. The exchange-correlation effects are incorporated within the von Barth-Hedin LSD approximation.³⁵ In this work, we have used fcc lattice constants of Ni, $\text{Ni}_{75}\text{Cu}_{25}$, and $\text{Ni}_{75}\text{Co}_{25}$ obtained by minimizing the total energy within the KKR-CPA framework for the ferromagnetic ground state. The final values used are: Ni, 6.594 a.u.; $\text{Ni}_{75}\text{Cu}_{25}$, 6.660 a.u.; and $\text{Ni}_{75}\text{Co}_{25}$, 6.567 a.u. These values are quite close to the corresponding experimental values of 6.6595, 6.7024, and 6.6694 a.u. from Ref. 36. Our computations thus yield unique LSD predictions and are parameter-free; the muffin-tin model is of course invoked implicitly, but this model is expected to provide a reasonable approximation to the crystal potential in close-packed systems.

Some specific computational details are as follows. The KKR-CPA charge- and spin-self-consistency cycles were carried out in the complex energy plane using an elliptic contour with 48 energy points, and a maximum angular-momentum cutoff $l_{\text{max}}=2$. The KKR-CPA equation was solved at all energies to a high accuracy so that the final spin-dependent crystal potential was converged to 1 mRy. The momentum density $n(\mathbf{p})$ was computed using the formulae given in Ref. 33 in terms of the momentum matrix elements of the KKR-CPA Green function. In order to obtain the Compton profiles accurately, $n(\mathbf{p})$ was computed on a mesh containing $48 \times 1183 \times 1291$ \mathbf{p} points. This mesh involves 1183 \mathbf{k} points in the 1/48th irreducible part of the Brillouin zone, each \mathbf{k} point being translated into 1291 \mathbf{p} points by adding lattice vectors, and the factor of 48 accounts for the symmetry operations of the point cubic group. The tetrahedral method of Lehman and Taut³⁷ was used to obtain the two-dimensional integrals of $n(\mathbf{p})$ necessary for evaluating the Compton profiles. The final CP's have been computed along the three low-index directions over 200 p_z points in the range 0–13 a.u. for the majority as well as minority spins, and are accurate to 0.001. The Lam-Platzman correction³⁸ is included in the computations using the occupation number density for the uniform electron gas.

III. EXPERIMENTAL DETAILS

The single crystals of $\text{Ni}_{75}\text{Cu}_{25}$ and $\text{Ni}_{75}\text{Co}_{25}$ were grown by the Bridgman method from melts containing high-purity components of nominal compositions. By using Laue x-ray-diffraction patterns to orient the crystals, three disk-shaped specimens (diameters 11.0 mm and 15.9 mm for $\text{Ni}_{75}\text{Cu}_{25}$ and $\text{Ni}_{75}\text{Co}_{25}$, respectively) with surface normals along the [100], [110], and [111] directions were cutoff by a spark erosion machine for each alloy. The samples were then thinned down to a thickness of 2.0 mm and polished chemically. The orientations were checked again via Laue diffraction, and found to be accurate to within 1.5°. From the observed spreads of the dots in the Laue patterns, we judge our single crystals to be of good quality, and to possess little short-range order.^{39,40} We refer the reader to Ref. 41 for many of the details of our Compton spectrometer using ^{137}Cs and ^{198}Au sources, and our data handling procedures. Some improvements were however made in connection with the present experiments. The older scattering chamber could not be evacuated when the ^{137}Cs source was in operation due to radiation protection of the source (the sample and the source were in the same chamber). We have therefore constructed a separate evacuable chamber for working with the ^{137}Cs source, whose dimensions ($300 \times 300 \times 1100$ mm³) are smaller than those of the older construction. The scattering geometry did not change much; the scattering angle was decreased from 167° to 165°, while the source-to-sample and source-to-detector distances of 422 mm and 281 mm, respectively, and the collimation system are almost the same as in the older setup. Special care was taken to shield the detector from the natural background. Also, two additional windows for measurements with 90° scattering angle were installed in the chamber. Remaining physical parameters (momentum

TABLE I. Parameters of the experiment.

γ energy of the source	661.65 keV
Activity of the source	85 Ci
Source dimensions	$\Phi = 11$ mm $h = 15$ mm
The distances;	
source sample	422 mm
sample detector	666 mm
source detector	281 mm
Scattering angle	165°
Diameter of primary beam at the sample position	15 mm
Detector (ORTEC, type GLP)	HP-Ge $\Phi = 16$ mm depth = 10 mm
Detector window	$\Phi = 12$ mm
The channel width of multichannel analyzer	57 eV
Resolution:	
detector	0.34 a.u.
geometrical	0.21 a.u.
total	0.40 a.u.
Measuring time	≈ 320 h for a sample
Counts at the maximum of Compton peak for NiCu sample (for NiCo multiply it by factor of 2)	$\approx 0.24 \cdot 10^6$ counts
Signal-to-background ratio for NiCu sample (for NiCo multiply it by factor of 2)	98:1

resolution, detector efficiency, etc.) did not change significantly, and can be found in Ref. 41 and are summarized in Table I.

The scope of the experimental work reported in this paper is limited to the investigation of directional differences of CP's in $\text{Ni}_{75}\text{Cu}_{25}$ and $\text{Ni}_{75}\text{Co}_{25}$. The reason is that our use of the high-energy source yields an additional background in the spectra, which makes the interpretation of absolute profiles difficult. The problem was discussed in Ref. 42 under the assumption that this background arises from bremsstrahlung radiation emitted from the sample. Subsequent analysis, including a series of long test experiments with the primary beam, indicates however that the aforementioned bremsstrahlung mechanism is unlikely to be sufficient to account for the observed background intensity. We estimate the level of the aforementioned background in the present measurements (for either alloy studied) to be $\approx 9\%$ of the single scattering events over the range -10 to $+10$ a.u. This background appears mainly on the low-energy side of the Compton peak. Apparently, the source itself emits unwanted extra radiation through some sort of a multiple-scattering process; a simulation of such an effect is difficult, if not impossible, since the chemical composition of our source is not well-known. Small angle scattering in the collimating system may also be responsible for some contamination of the beam. In any event, the high-energy side of the Compton peak appears to be "cleaner;" the anisotropies (directional differences) determined from the left and the right sides of the measured CP's are the same within experimental error. Accordingly, the final data presented here uses the full measured CP's in order to improve the statistical accuracy of the difference data.

Bearing all this in mind, and the fact that the background appears to be essentially isotropic, much more reliable infor-

mation can be drawn from directional anisotropies that are expected to be insensitive to such uncertainties in the absolute profiles; the question of the nature of the background will be taken up elsewhere. We emphasize in this connection that the diameter and thickness of the three specimens for each of the two alloys investigated were practically the same. Therefore, the systematic effect of multiple scattering in the alloy needed to be calculated only once for all three crystal orientations. The Monte Carlo simulations showed that multiple-scattering events amount to 18% and 22% of the single-scattering events (over the momentum range -10 a.u. to $+10$ a.u.) for $\text{Ni}_{75}\text{Cu}_{25}$ and $\text{Ni}_{75}\text{Co}_{25}$, respectively. This multiple-scattering contribution was subtracted from the measured CP's that were then renormalized to the total area (number of electrons) under the theoretical profiles over the aforementioned momentum range before obtaining directional differences.

Only the ^{137}Cs source was used in the present experiments. The ^{198}Au source could presumably yield somewhat better absolute profiles, but little improvement with respect to the directional anisotropies could be expected; see discussion of Ag data.⁴² Keeping in mind our focus on the directional anisotropies, and the high cost of the irradiation of the ^{198}Au source, the measurements were limited to the ^{137}Cs source.

IV. RESULTS AND DISCUSSION

A. Ferromagnetic electronic structures

Figures 1–4 show selected results for spin-dependent densities of states (DOS's), the site-dependent component densities of states (CDOS's), and the partial contributions from different angular momenta (PDOS's) in Ni, $\text{Ni}_{75}\text{Co}_{25}$ and

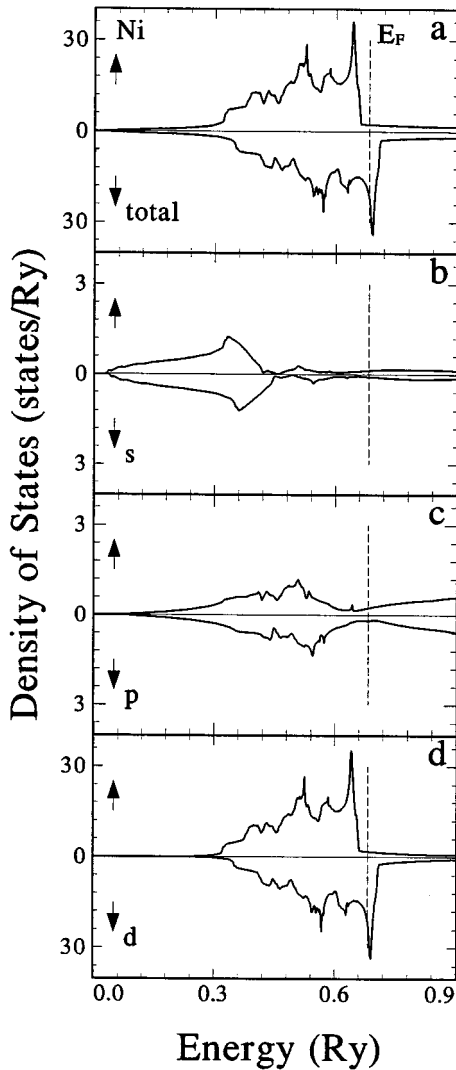


FIG. 1. Self-consistent density of states for ferromagnetic Ni. The up (down) arrows denote the majority (minority) spin components of various quantities. (a) gives the total density of states. (b)–(d) give the s , p , and d angular-momentum contributions to the total density of states. Dashed vertical lines denote the Fermi energy E_F . Note scale changes in different panels.

$\text{Ni}_{75}\text{Cu}_{25}$. The changes in the electronic structure of Ni with the addition of Co or Cu can be delineated with reference to these figures.

The majority (up) and minority (down) DOS's in Ni possess very similar shapes (Fig. 1), although the width of the minority spin band is somewhat larger. The addition of Co to Ni induces little change in the up-spin DOS aside from a general smoothing of all features reflecting disorder smearing of states, Fig. 2. In contrast, the down-spin DOS's in Ni and $\text{Ni}_{75}\text{Co}_{25}$ differ sharply, and the down-spin Ni peak at ≈ 0.7 Ry (Fig. 1) is substantially broadened in the alloy; this peak is more pronounced and lies at a higher energy (≈ 0.75 Ry) in the Co-CDOS, compare Figs. 3(a1) and 3(b1).

These results give insight into how magnetic moments form on Co and Ni atoms in the alloy. The up-spin d band is full in the Ni-as well as the Co-CDOS. But, for down-spins, the high-energy peak in the Co-CDOS is essentially empty,

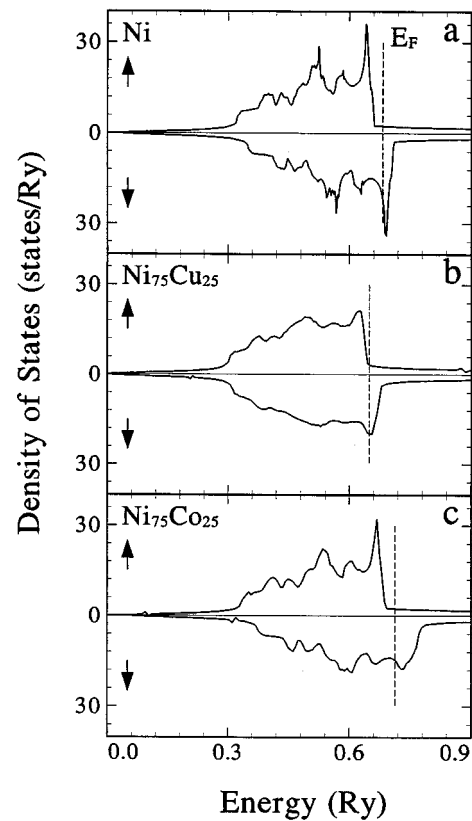


FIG. 2. Self-consistent KKR-CPA density of states in, Ni (a), $\text{Ni}_{75}\text{Cu}_{25}$ (b), and $\text{Ni}_{75}\text{Co}_{25}$ (c). Meaning of arrows and the vertical dashed lines is same as in the caption to Fig. 1.

while in the Ni-CDOS this peak is only partially empty, leading to a substantially higher moment on Co atoms. Our computations show that in $\text{Ni}_{75}\text{Co}_{25}$, Co possesses a moment of $1.63 \mu_B/\text{atom}$, and Ni of $0.64 \mu_B/\text{atom}$; the latter is close to our calculated moment of $0.62 \mu_B/\text{atom}$ in fcc Ni. The replacement of a Ni atom by a Co atom in the alloy thus contributes a net moment of about $1 \mu_B$. In other words, the reduced valence of Co is accommodated almost completely via the depletion of down-spin electrons. The present KKR-CPA predictions for $\text{Ni}_{75}\text{Co}_{25}$ thus follow the simple Slater-Pauling curve⁴³ for the total magnetic moment of the alloy.

The computed Ni and Co moments quoted in the preceding paragraph are in reasonable accord with the measured values.⁴⁴ Briefly, a detailed analysis of the magnetic form factors in Ref. 45 shows that the spin moments of NiCo alloys vary linearly with composition, and that the individual moments are $\text{Ni}=0.526 \mu_B$, $\text{Co}=1.66 \mu_B$, assuming no conduction electron ($4s$) polarization. Reference 46 deduces Ni moments of $0.617(16) \mu_B$ and $-0.091(16) \mu_B$ for $3d$ and $4s$ electrons, and postulates a $3d$ Co moment of $1.7 \mu_B$. Reference 47 obtains a $4s$ moment in $\text{Ni}_{75}\text{Co}_{25}$ of $-0.074(23) \mu_B$. Combining these results, one obtains total spin only moments of $0.526(23) \mu_B$ and $1.63(2) \mu_B$ for Ni and Co atoms in NiCo alloys, comparable to our corresponding computed values of 0.64 and $1.63 \mu_B$.^{48,49} The close agreement between the measured and computed Co moment is probably fortuitous—the discrepancy for the Ni moment is perhaps more representative of the sort of uncertainties inherent in first-principles comparisons of this sort.

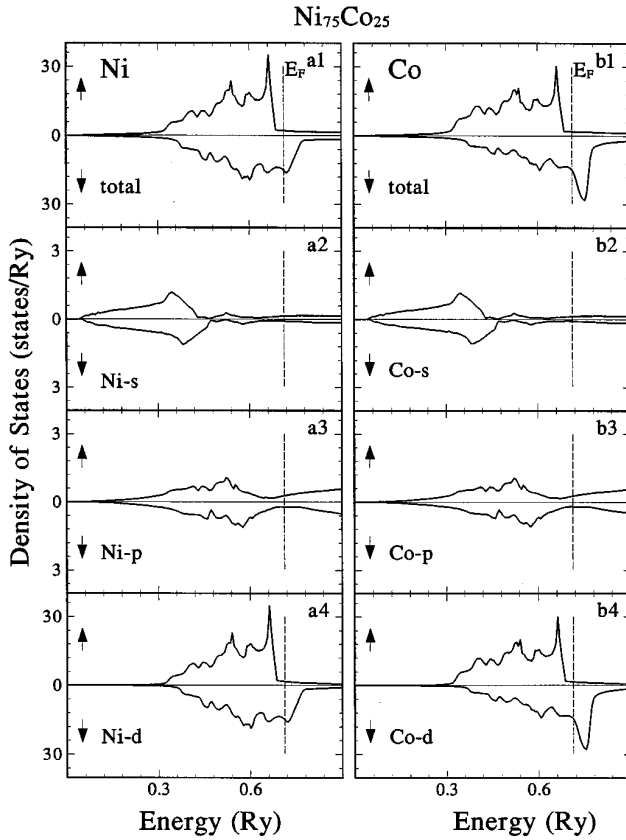


FIG. 3. Site-dependent KKR-CPA densities of states in $\text{Ni}_{75}\text{Co}_{25}$. Ni and Co components are given in left and right figures, respectively. The total density associated with Ni or Co sites is shown further broken up into angular-momentum components. Meaning of arrows and the vertical dashed lines is same as in the caption to Fig. 1.

The situation with NiCu alloys is quite different. In contrast to $\text{Ni}_{75}\text{Co}_{25}$, the up- and down-spin DOS's in $\text{Ni}_{75}\text{Cu}_{25}$ possess similar shapes, Fig. 2; this is, in fact, true of both the Ni-as well as the Cu-CDOS's, Fig. 4. Cu impurities in Ni are nonmagnetic, and yield a fairly broad *d* resonance centered around 0.4 Ry [Fig. 4(b4)]. (Interestingly, Ni impurities in Cu yield a more localized virtual bound state.) The average moment in $\text{Ni}_{1-x}\text{Cu}_x$ collapses with increasing *x* for two reasons. First, the exchange splitting on Ni sites decreases in the alloy [Fig. 4(a1)]; the calculated Ni moment in $\text{Ni}_{75}\text{Cu}_{25}$ is $0.41 \mu_B/\text{atom}$ compared to the value of $0.62 \mu_B/\text{atom}$ in Ni.^{50,51} Second, there is a dilution effect due to the addition of nonmagnetic Cu atoms; as a result, the average moment in $\text{Ni}_{75}\text{Cu}_{25}$ is $0.30 \mu_B/\text{atom}$. Note that in NiCo alloys the Ni and Co moments are nearly concentration-independent, so that changes in the average moment arise from the replacement of Ni by the larger Co moments.

It is noteworthy that alloying Ni with either Co or Cu mostly influences *d* states, with the *s* or *p* states undergoing little change, see Figs. 3 and 4. In fact, upon integrating the PDOS's of Figs. 3 and 4 up to the Fermi energy, we find that the total number of *s* or *p* electrons on Ni, Co, and Cu sites in Ni, $\text{Ni}_{75}\text{Co}_{25}$, and $\text{Ni}_{75}\text{Cu}_{25}$ is essentially the same.

The preceding theoretical results are in good overall accord with the picture of magnetism of Ni-based alloys that

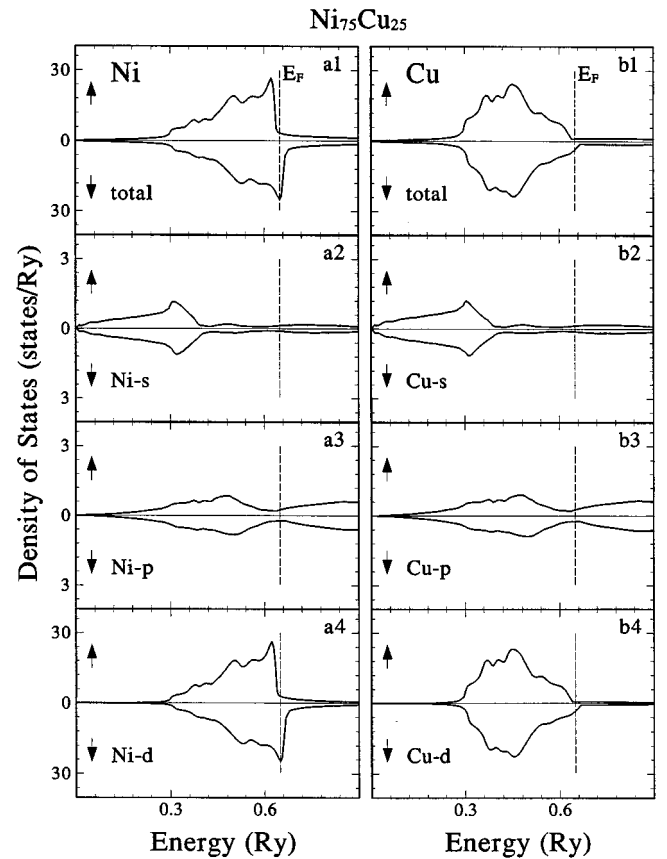


FIG. 4. Same as the caption to Fig. 3, except that this figure refers to $\text{Ni}_{75}\text{Cu}_{25}$.

has been adduced from various model studies starting with the early work of Friedel, followed by Kanamori and others.^{52,53} In particular, the repulsive Coulomb interaction on the Co sites is seen to produce a virtual bound statelike structure above the Fermi energy in the minority spin DOS in Fig. 3, while the majority-spin DOS of Ni is hardly affected by adding Co.

B. Spin-resolved theoretical Compton profiles

As expected, the overall shapes of the Compton profiles in Ni, $\text{Ni}_{75}\text{Co}_{25}$, and $\text{Ni}_{75}\text{Cu}_{25}$ are quite similar, see Fig. 5 for typical results. It is more interesting to analyze fine structure in the spectra. For this purpose, we consider the anisotropies of Figs. 6–8, obtained by taking differences of the Compton profiles along the three high-symmetry directions. The contributions of the majority and minority spin states are shown separately in order to delineate the role of magnetism in the evolution of the Compton spectra of the alloys.

The maximum total anisotropy in Ni is seen from Figs. 6 and 5 to be about 2% of the peak height. $J_{110}-J_{100}$ and $J_{111}-J_{110}$ anisotropies are generally larger compared to the $J_{111}-J_{100}$ case; this results from the fact that the [110] profile possesses a more pronounced fine structure, while the [111] and [100] profiles are rather similar in shape. The majority and minority contributions to the anisotropy are seen to differ substantially in the low-momentum range of *p* less than about 1 a.u. For example, the sharp dip around 0.6 a.u. in the spin-down anisotropy in Fig. 6(a) is essentially miss-

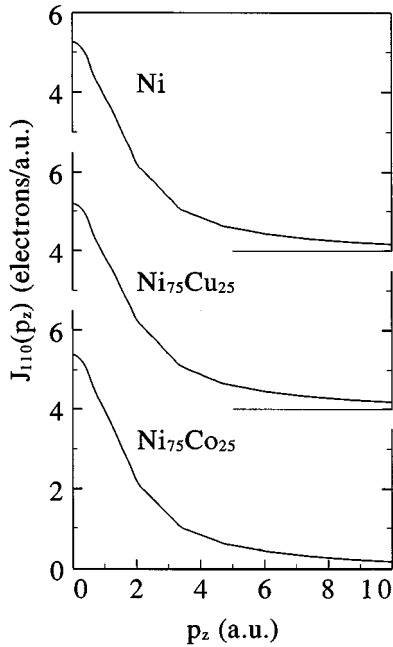


FIG. 5. Theoretical Compton profiles J_{110} as a function of momentum transfer p_z along the [110] direction, in Ni, Ni₇₅Cu₂₅, and Ni₇₅Co₂₅.

ing in the majority-spin case; similarly, at $p_z=0$ in Fig. 6(c), the spin-up curve is positive and decreasing while the spin-down curve is negative and increasing. There are notable differences at higher momenta as well; in Fig. 6(a), the down-spin features around 1–2 a.u. and 2.4–3.2 a.u. possess more fine structure compared to the up-spin anisotropies, and the down-spin dips around 3.4, 4.8, and 6 a.u. are virtually missing in the up-spin case. In this vein, the structures in Fig. 6(c) are also seen to differ in their shapes, positions, and amplitudes for the majority and minority spins. In understanding these results, recall that the underlying up- and down-spin DOS's in Ni are quite similar (Fig. 1). But, the up-spin d bands are full, while the down-spin d bands contain holes, yielding a more complex down-spin Fermi surface with many sheets. Therefore, we should expect the down-spin momentum density to be more structured, and the associated anisotropy to be generally larger than for the up-spins. The preceding discussion also makes it clear that a proper description of the Compton profile of Ni requires the inclusion of ferromagnetic ordering in the computations.

We have compared our computed directional anisotropies in the Ni CP's with other available experimental and theoretical results in the literature.^{19–21,23,26–29,54} We also considered the [100] and [111] magnetic CP's of Ref. 29 measured at a relatively low-momentum resolution of 0.7 a.u. [full width at half maximum (FWHM)], and the corresponding theoretical profiles of Ref. 28. Overall, our theoretical anisotropies as well as the magnetic profiles of Ni are quite consistent with the previously published work, and for this reason and the fact that Ni is not the focus of this article, we avoid getting into the details of these comparisons.

We turn now to discuss the effects of alloying on the Compton profile of Ni. Recall that the Ni up-spin states are influenced relatively little by the addition of either Co or Cu

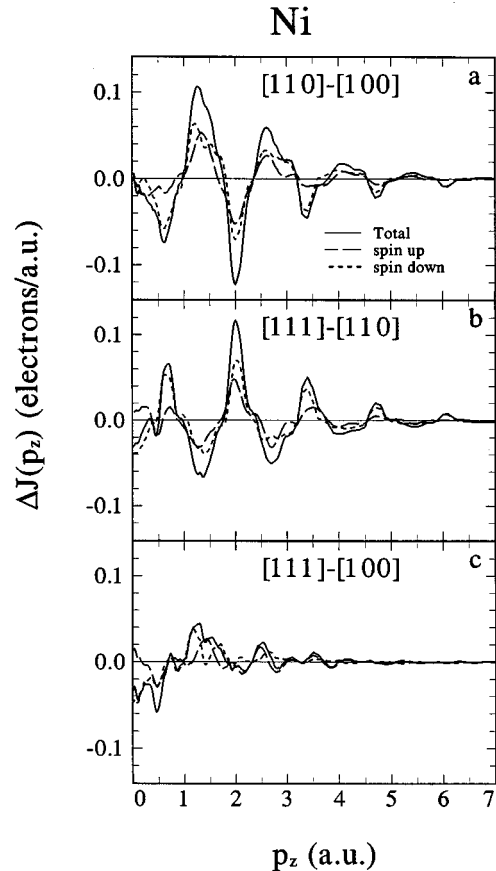


FIG. 6. Theoretical anisotropic profiles in Ni. Differences in Compton profiles along various pairs of high-symmetry directions are shown. The total anisotropy (solid) is decomposed into the majority (up, dashed), and minority (down, dotted) contributions.

and, in particular, the up-spin d bands remain filled in Ni₇₅Co₂₅ as well as Ni₇₅Cu₂₅ (Fig. 2). This is the reason that the up-spin anisotropies in Ni₇₅Co₂₅ (Fig. 7) and Ni₇₅Cu₂₅ (Fig. 8) are virtually indistinguishable from the corresponding Ni results of Fig. 6. The down-spin states, on the other hand, undergo substantial modifications, as already pointed out in connection with Figs. 2–4 above. Therefore, in examining the effects of alloying on the Compton profile of Ni here, we need not consider the up-spin contribution further, and can focus our attention on just the *down-spin* contribution, or equivalently on the total profiles.

A reference to Figs. 6 and 7 shows that the down-spin density better resembles the up-spin density in Ni₇₅Cu₂₅ compared to Ni; for example, the complicated down-spin structure between 1–2 a.u. in Ni [Fig. 6(a)] is replaced by a broad hump in Ni₇₅Cu₂₅ [Fig. 7(a)]. Two effects are at work here. First, the disorder induced smearing of states in the alloy will smooth sharp structures related to Fermi surfaces, and thus tend to decrease momentum density anisotropies. Second, since the addition of Cu to Ni causes a decrease in the average magnetic moment, we expect the differences between the up- and down-spin densities to decrease generally upon alloying. Note however that the aforementioned effects do not take place uniformly as a function of momentum, e.g., the down-spin dips at 0.6 and 3.3 a.u. in Fig. 7(a) continue to be quite prominent in Ni₇₅Cu₂₅.

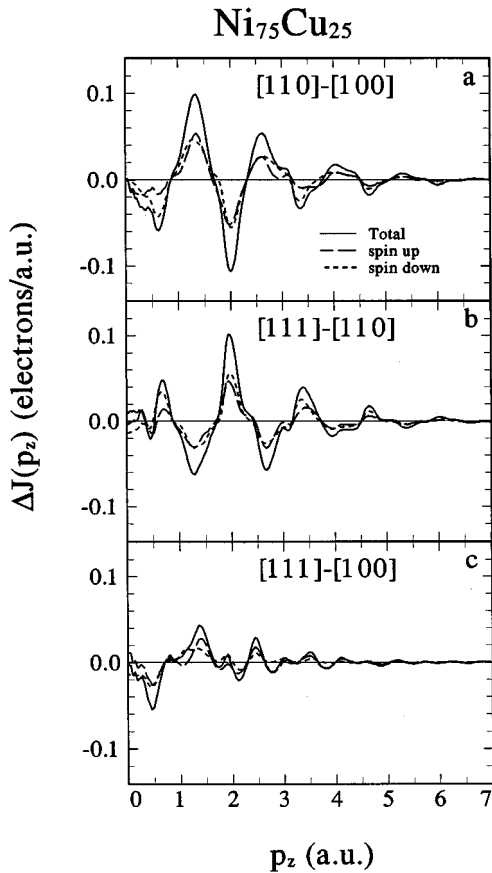


FIG. 7. Same as the caption to Fig. 6, except that this figure refers to $\text{Ni}_{75}\text{Cu}_{25}$.

These considerations also allow us to understand the results for $\text{Ni}_{75}\text{Co}_{25}$ (Fig. 8). The situation is somewhat more complicated compared to $\text{Ni}_{75}\text{Cu}_{25}$ because here the magnetic moment in the alloy is larger than in Ni. Therefore, the splitting between the up- and down-spin densities of Ni will *increase* upon alloying with Co. The effect of disorder smearing, on the other hand, still tends to reduce anisotropies generally in the alloy. The net effect then is that some features in the alloy become more prominent in the down-spin density, while others are less so. For example, the difference between the up- and down-spin anisotropies at $p_z=0$ is larger in $\text{Ni}_{75}\text{Co}_{25}$ than in Ni (compare corresponding panels in Figs. 6 and 8); in contrast, this splitting in the dips at 2 and 4.7 a.u. in Ni [Fig. 6(a)] is smaller in $\text{Ni}_{75}\text{Co}_{25}$ [Fig. 8(a)]. The reader can observe such effects at other momenta from Figs. 6 and 8.

C. Comparison with experiments

The theoretical anisotropies are presented together with the experimental results in Figs. 9 and 10. A good overall accord is seen in comparing the resolution broadened theoretical spectra (solid) with the corresponding experimental data. The agreement for the [111]-[100] anisotropy in both $\text{Ni}_{75}\text{Cu}_{25}$ [Fig. 9(c)] and $\text{Ni}_{75}\text{Co}_{25}$ [Fig. 10(c)] is striking, although there is a difference around $p_z=0$ in Fig. 10(c). The shapes of the undulations in the [110]-[100] [Figs. 9(a), 10(a)] as well as the [111]-[110] anisotropies [Figs. 9(b),

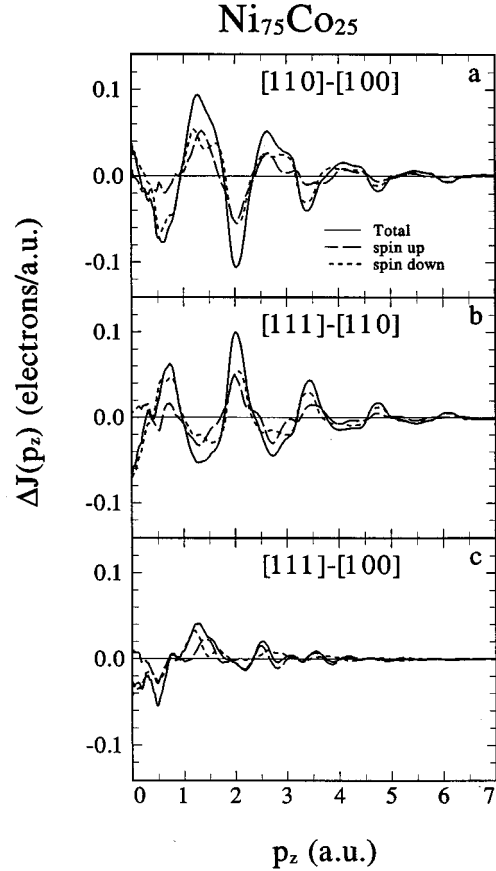


FIG. 8. Same as the caption to Fig. 6, except that this figure refers to $\text{Ni}_{75}\text{Co}_{25}$.

10(b)] are similar, but the theoretical amplitudes are higher; this discrepancy is not unexpected and has been pointed out frequently in the literature, and is due presumably to the electron correlation effects beyond the local-density approximation missing in the present computations.^{5–8} Notably, near $p_z=0$ in $\text{Ni}_{75}\text{Cu}_{25}$, the computed [110]-[100] anisotropy is smaller [Fig. 9(a)], while the [111]-[110] anisotropy is larger [Fig. 9(b)] than the measurements. Although the reasons for these differences are unclear, they may reflect, for example, effects of clustering and short-range ordering in the alloy beyond the random approximation implicit in the KKR-CPA framework employed in our calculations.

A comparison of the broadened and unbroadened theory curves in Figs. 9 and 10 shows that the resolution of 0.4 a.u. smooths out much of the fine structure in the spectra discussed in connection with Figs. 6–8 above. Further, little difference can be seen between the theoretical anisotropies in $\text{Ni}_{75}\text{Cu}_{25}$ and $\text{Ni}_{75}\text{Co}_{25}$ after broadening, aside from the region near $p_z=0$. A higher experimental resolution is necessary in order to delineate differences in the electronic structure and bonding of the present alloys via the Compton technique.

Careful intercomparisons of the anisotropies from well-characterized samples of Ni, $\text{Ni}_{75}\text{Cu}_{25}$, and $\text{Ni}_{75}\text{Co}_{25}$ should prove interesting. Keeping in mind that changes in the Compton profile of Ni arise mainly from those in the minority spins, theoretically predicted spectral features that bear particular attention are: (i) Changes near $p_z=0$, e.g., the

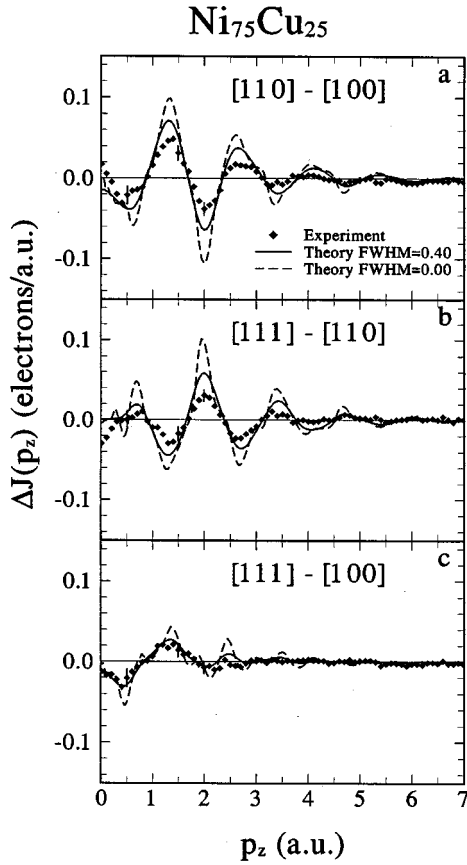


FIG. 9. Comparison of theoretical and experimental anisotropies in $\text{Ni}_{75}\text{Cu}_{25}$. Solid lines give theoretical results that include resolution broadening of 0.4 a.u. (FWHM); theoretical results before folding in the resolution are shown dashed.

[110]-[100] anisotropy in Ni is predicted to increase on adding Co, but to decrease on adding Cu [Figs. 6(a), 7(a), 8(a)]; (ii) The [110]-[100] down-spin feature between 1–1.8 a.u. in Ni possesses a prominent peak around 1.2 a.u. and two smaller peaks at higher momenta [Fig. 6(a), dotted]; this is replaced by essentially a single broader peak in $\text{Ni}_{75}\text{Cu}_{25}$ [Fig. 7(a)] and by two peaks around 1.2 and 1.6 a.u. in $\text{Ni}_{75}\text{Co}_{25}$ [Fig. 8(a)]; (iii) The [110]-[100] down-spin feature between 2.4 and 3.2 a.u. in Ni consists of a peak around 2.6 a.u. and roughly a knee at higher momentum; in $\text{Ni}_{75}\text{Cu}_{25}$, the amplitude of the knee decreases, but in $\text{Ni}_{75}\text{Co}_{25}$, the knee turns into a prominent peak. Notably, our computations suggest that in the special cases of the present alloys, by subtracting the alloy profiles from the corresponding Ni profiles (after proper background corrections and normalization), one should obtain a measure of the changes in only the *down-spin* profiles.

V. SUMMARY AND CONCLUSIONS

We have presented ferromagnetic electronic structures and spin-resolved Compton profiles along the three high-symmetry directions in $\text{Ni}_{75}\text{Cu}_{25}$ and $\text{Ni}_{75}\text{Co}_{25}$ disordered alloys employing the framework of the KKR-CPA theory, and treating correlation effects within the LSD scheme. Corresponding computations on ferromagnetic Ni were also carried out. A high level of charge- and spin-self-consistency

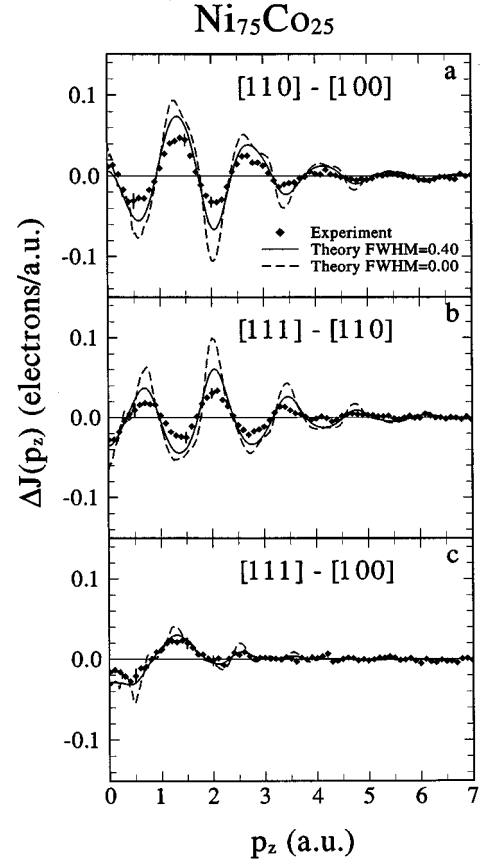


FIG. 10. Same as the caption to Fig. 9, except that this figure refers to $\text{Ni}_{75}\text{Co}_{25}$.

was achieved in all cases. The results are parameter-free in that they are based on lattice constants determined by minimizing the total energy. On the experimental side, we have presented the [100], [110], and [111] Compton profiles from single crystals of $\text{Ni}_{75}\text{Cu}_{25}$ and $\text{Ni}_{75}\text{Co}_{25}$ using a ^{137}Cs γ -ray source.

Our computations show that the majority-spin spectrum of Ni undergoes relatively small changes upon the addition of Cu or Co impurities, and that the majority states continue to be essentially completely occupied in $\text{Ni}_{75}\text{Cu}_{25}$ as well as $\text{Ni}_{75}\text{Co}_{25}$, as is the case in Ni. Concomitantly, the majority-spin contribution to the Compton profiles in Ni, $\text{Ni}_{75}\text{Cu}_{25}$ and $\text{Ni}_{75}\text{Co}_{25}$ is also nearly the same. The spectral changes in the alloys are thus limited mainly to the minority-spin states. The Co atoms in Ni possess a moment of $1.63 \mu_B$ while Ni atoms continue to possess a moment of $0.64 \mu_B$ in NiCo alloys, so that the average moment per unit cell increases from $0.60 \mu_B$ in Ni to $0.86 \mu_B$ in $\text{Ni}_{75}\text{Co}_{25}$ as Ni atoms are replaced by Co atoms of higher moments. On the other hand, Cu impurities that remain nonmagnetic in Ni, cause a reduction in the Ni moment as well, and the net moment in $\text{Ni}_{75}\text{Cu}_{25}$ decreases to $0.30 \mu_B$ per unit cell with $0.41 \mu_B$ on Ni.

In comparing theoretical and experimental profiles, we focus on anisotropies defined by taking differences in the Compton profiles along various directions. The absolute values of the experimental profiles in the present measurements are difficult to interpret due to the presence of a background contribution of uncertain origin; further work in understand-

ing this background is necessary before direct comparisons between the measured and calculated absolute profiles can be undertaken. The overall agreement between theory and experiment with respect to the $J_{111}-J_{100}$, $J_{111}-J_{110}$, and $J_{110}-J_{100}$ anisotropies in $\text{Ni}_{75}\text{Cu}_{25}$ as well as $\text{Ni}_{75}\text{Co}_{25}$ is reasonable. The amplitudes of the undulations in the measured anisotropies are smaller than the computations, due presumably to the effects of correlations beyond the LSD missing in our theoretical framework; there also are some discrepancies around $p_z=0$ whose origin is unclear.

We show clearly that a broadening of 0.4 a.u. (FWHM) leads to washing out of much of the fine structure in the computed directional anisotropies. In this connection, we identify a number of specific signatures of the Cu and Co impurities on the directional anisotropies of $\text{Ni}_{75}\text{Cu}_{25}$ and $\text{Ni}_{75}\text{Co}_{25}$. The higher momentum resolution of the synchrotron light sources should allow a delineation of these interesting effects, and cast the discrepancies between theory and

experiment in a clearer light. Our computations show that changes in the directional anisotropies of Ni when alloyed with Cu or Co are representative of changes *only* in the minority-spin contribution to the total profiles. This curious circumstance comes about because, as already noted, the majority-spin contributions are nearly the same in Ni, $\text{Ni}_{75}\text{Cu}_{25}$, and $\text{Ni}_{75}\text{Co}_{25}$.

ACKNOWLEDGMENTS

This work is supported by the U.S. Department of Energy under Contract No. W-31-109-ENG-38, including a subcontract to Northeastern University, a travel grant from NATO, the Polish Council of Science and Research through Grant Nos. 2-P03B-061-08 and 2-0182-91-01, and the allocation of supercomputer time at the NERSC and Pittsburgh Supercomputer Centers.

- ¹A. Bansil, *Z. Naturforsch. Teil A* **48A**, 165 (1993).
- ²L. Dobrzyński, *Z. Naturforsch. Teil A* **48A**, 266 (1993).
- ³B. G. Williams, *Compton Scattering* (McGraw-Hill, New York, 1977).
- ⁴M. J. Cooper, *Rep. Prog. Phys.* **48**, 415 (1985).
- ⁵Y. Sakurai, Y. Tanaka, A. Bansil, S. Kaprzyk, A. T. Stewart, Y. Nagashima, T. Hyodo, S. Nanao, H. Kawata, and N. Shiotani, *Phys. Rev. Lett.* **74**, 2252 (1995).
- ⁶W. Schülke, G. Stutz, F. Wohlert, and A. Kaprolat, *Phys. Rev. B* **54**, 14 381 (1996).
- ⁷K. Hämäläinen, S. Manninen, C.-C. Kao, W. Caliebe, J. B. Hastings, A. Bansil, S. Kaprzyk, and P. M. Platzman, *Phys. Rev. B* **54**, 5453 (1996).
- ⁸M. Itou, Y. Sakurai, T. Ohata, A. Bansil, S. Kaprzyk, Y. Tanaka, H. Kawata, and N. Shiotani, *J. Phys. Chem. Solids* (to be published).
- ⁹S. Kaprzyk, *Acta Phys. Pol. A* **91**, 135 (1997).
- ¹⁰P. E. Mijnarends and A. Bansil, in *Positron Spectroscopy of Solids*, Proceedings of the International School of Physics "Enrico Fermi," Course CXXV, Varenna, 1993, edited by A. Dupasquier and A. P. Mills (IOS Press, Amsterdam, 1995).
- ¹¹A. Bansil, in *Positron Annihilation*, edited by P. G. Coleman, S. G. Sharma, and L. M. Diana (North-Holland, Amsterdam, 1982), p. 273.
- ¹²A. Bansil and P. E. Mijnarends, *Phys. Rev. B* **30**, 628 (1984).
- ¹³A. Bansil, S. Kaprzyk, and J. Tobola, *Mater. Res. Soc. Symp. Proc.* **253**, 505 (1992).
- ¹⁴P. E. Mijnarends and A. Bansil, *Phys. Rev. B* **19**, 2912 (1979).
- ¹⁵R. Benedek, R. Prasad, S. Manninen, B. K. Sharma, A. Bansil, and P. E. Mijnarends, *Phys. Rev. B* **32**, 7650 (1985).
- ¹⁶Y. Nakao and S. Wakoh, *J. Phys. Soc. Jpn.* **51**, 2847 (1982).
- ¹⁷S. S. Rajput, R. Prasad, R. M. Singru, W. Triftshäuser, A. Eckert, G. Kögel, S. Kaprzyk, and A. Bansil, *J. Phys.: Condens. Matter* **5**, 6419 (1993).
- ¹⁸S. Kaprzyk and A. Bansil (unpublished).
- ¹⁹P. Eisenberger and W. A. Reed, *Phys. Rev. B* **9**, 3242 (1974).
- ²⁰P. Pattison, N. K. Hansen, and J. R. Schneider, *Z. Phys. B* **46**, 285 (1982).
- ²¹A. J. Rollason, J. R. Schneider, D. S. Laundy, R. S. Holt, and M. J. Cooper, *J. Phys. F* **17**, 1105 (1987).
- ²²R. Richter, H. Eschrig, and B. Velicky, *J. Phys. F* **17**, 351 (1987).
- ²³D. L. Anastassopoulos, G. D. Priftis, N. I. Papanicolaou, N. C. Bacalis, and A. Papaconstantopoulos, *J. Phys.: Condens. Matter* **3**, 1099 (1991).
- ²⁴G. E. Bauer and J. R. Schneider, *Z. Phys. B* **54**, 17 (1983).
- ²⁵G. E. Bauer and J. R. Schneider, *Phys. Rev. Lett.* **52**, 2061 (1984).
- ²⁶G. E. Bauer and J. R. Schneider, *J. Phys. Chem. Solids* **45**, 675 (1984).
- ²⁷V. Sundararajan, R. Asokamani, and D. G. Kanhere, *Phys. Rev. B* **38**, 12 653 (1988).
- ²⁸V. Sundararajan and D. G. Kanhere, *J. Phys.: Condens. Matter* **3**, 3311 (1991).
- ²⁹D. N. Timms, A. Brahmia, M. J. Cooper, S. P. Collins, S. Hamouda, D. Laundy, C. Kilbourne, and M.-C. Saint Lager, *J. Phys.: Condens. Matter* **2**, 3427 (1990).
- ³⁰A. Bansil, *Phys. Rev. Lett.* **41**, 1670 (1978); *Phys. Rev. B* **20**, 4035 (1979).
- ³¹B. E. A. Gordon, W. E. Temmerman, and B. L. Gyorffy, *J. Phys.: Condens. Matter* **11**, 821 (1981); *Z. Szotek, B. L. Gyorffy, G. M. Stocks, and W. M. Temmerman, J. Phys. F* **14**, 2571 (1991).
- ³²S. Kaprzyk and A. Bansil, *Phys. Rev. B* **42**, 7358 (1990); A. Bansil and S. Kaprzyk, *ibid.* **43**, 10 335 (1991).
- ³³P. E. Mijnarends and A. Bansil, *Phys. Rev.* **13**, 2381 (1976).
- ³⁴A. Bansil, R. S. Rao, P. E. Mijnarends, and L. Schwartz, *Phys. Rev. B* **23**, 3608 (1981).
- ³⁵U. von Barth and L. Hedin, *J. Phys. C* **5**, 1629 (1972); A. K. Rajagopal and J. Callaway, *Phys. Rev. B* **7**, 1912 (1973).
- ³⁶W. B. Pearson, *Handbook of the Lattice Spacing and Structures of Metals and Alloys* (Pergamon, London, 1958).
- ³⁷G. Lehman and M. Taut, *Phys. Status Solidi B* **54**, 469 (1972).
- ³⁸L. Lam and P. M. Platzman, *Phys. Rev. B* **9**, 5122 (1974).
- ³⁹A separate, laborious set of experiments would be needed in order to determine the short-range order parameters for our specimens. In the absence of such measurements, perhaps it is reasonable to assume that the degree of randomness in our specimens is typical and quite high. For example, very detailed experiments of Ref. 40 find in a $\text{Ni}_{0.475}\text{Cu}_{0.525}$ sample the first Cowley parameter

- of 0.121 with the others being at least one order of magnitude smaller. We are not aware of a similar study of NiCo alloys.
- ⁴⁰B. Mozer, D. T. Keating, and S. C. Moss, *Phys. Rev.* **175**, 868 (1968).
- ⁴¹A. Andrejczuk, E. Żukowski, L. Dobrzyński, and M. J. Cooper, *Nucl. Instrum. Methods Phys. Res. A* **337**, 133 (1993).
- ⁴²A. Andrejczuk, L. Dobrzyński, J. Kwiatkowska, F. Maniowski, S. Kaprzyk, A. Bansil, E. Żukowski, and M. J. Cooper, *Phys. Rev. B* **48**, 15 552 (1993).
- ⁴³S. Chikazumi, *Physics of Magnetism* (Wiley, New York, 1964).
- ⁴⁴We emphasize that all computed moments in this article refer to the total spin moment that includes all electrons.
- ⁴⁵B. Van Laar, F. Maniowski, S. Kaprzyk, and L. Dobrzyński, *Nukleonika* **25**, 835 (1980).
- ⁴⁶L. Dobrzyński, *Int. J. Magn.* **6**, 291 (1974).
- ⁴⁷B. Antonini, F. Menzinger, A. Paoletti, and F. Sacchetti, *Int. J. Magn.* **1**, 183 (1971).
- ⁴⁸The moments are in general temperature-dependent, and this effect should be accounted for in a detailed comparison between theory and experiment. For example, the total measured moment in Ni at room temperature is $0.579(5)\mu_B$, compared to the zero-temperature estimate of $0.612\mu_B$ (Ref. 49). Most experimental values refer to the room temperature, while our computations are at zero temperature.
- ⁴⁹S. Arajs and G. R. Dunmyre, *Phys. Status Solidi B* **21**, 191 (1967); R. Pauthenet, in *High Field Magnetism*, edited by M. Date (North-Holland, Amsterdam, 1983), p. 77.
- ⁵⁰This value is in reasonable accord with the experimental estimate of $0.46\mu_B$ per Ni atom in Ni₇₅Cu₂₅ at 0 K (Ref. 51).
- ⁵¹R. M. Bozorth, *Ferromagnetism* (Van Nostrand, Toronto, 1951).
- ⁵²J. Friedel, *Nuovo Cimento Suppl.* **8**, 287 (1958).
- ⁵³J. Kanamori, *J. Phys. (France)* **35**, C4 (1974); H. Hasegawa and J. Kanamori, *J. Phys. Soc. Jpn.* **33**, 1599 (1972).
- ⁵⁴G. E. Bauer and J. R. Schneider, *Phys. Rev. B* **31**, 681 (1985).